frontiers in Chemistry

ORIGINAL RESEARCH
published: 19 September 2018
doi: 10.3389/fchem.2018.00415

Adsorption and Photocatalytic Processes of Mesoporous SiO_2-Coated Monoclinic $BiVO_4$

Duangdao Channei[1,2]*, **Auppatham Nakaruk**[3,4], **Wilawan Khanitchaidecha**[4,5], **Panatda Jannoey**[6] and **Sukon Phanichphant**[7]

[1] Department of Chemistry, Faculty of Science, Naresuan University, Phitsanulok, Thailand, [2] Research Center for Academic Excellence in Petroleum, Petrochemicals and Advanced Materials, Naresuan University, Phitsanulok, Thailand, [3] Department of Industrial Engineering, Faculty of Engineering, Naresuan University, Phitsanulok, Thailand, [4] Centre of Excellence for Innovation and Technology for Water Treatment, Naresuan University, Phitsanulok, Thailand, [5] Department of Civil Engineering, Faculty of Engineering, Naresuan University, Phitsanulok, Thailand, [6] Department of Biochemistry, Faculty of Medical Science, Naresuan University, Phitsanulok, Thailand, [7] Materials Science Research Center, Faculty of Science, Chiang Mai University, Chiang Mai, Thailand

The silicon dioxide (SiO_2)–coated bismuth vanadate ($BiVO_4$) composites as visible–driven–photocatalysts were successfully synthesized by the co–precipitation method. The effects of SiO_2 coating on the structure, optical property, morphology and surface properties of the composites were investigated by X–ray diffraction (XRD), UV–visible diffuse reflectance spectroscopy (DRS), transmission electron microscopy (TEM) and Brunauer–Emmette–Teller (BET) measurements. The photocatalytic activity of monoclinic $BiVO_4$ and $BiVO_4/SiO_2$ composites were evaluated according to the degradation of methylene blue (MB) dye aqueous solution under visible light irradiation. The $SiO_{2–}$coated $BiVO_4$ composites showed the enhancing photocatalytic activity approximately threefold in comparison with the single phase $BiVO_4$.

Keywords: composite materials, photocatalysis, $BiVO_4$, BET isotherms, SiO_2

OPEN ACCESS

Edited by:
Hongqi Sun,
Edith Cowan University, Australia

Reviewed by:
Priyabrat Mohapatra,
C. V. Raman College of Engineering,
India
M. Nageeb Rashed,
Aswan University, Egypt

***Correspondence:**
Duangdao Channei
duangdaoc@nu.ac.th

Specialty section:
This article was submitted to
Green and Sustainable Chemistry,
a section of the journal
Frontiers in Chemistry

Received: 09 March 2018
Accepted: 23 August 2018
Published: 19 September 2018

Citation:
Channei D, Nakaruk A,
Khanitchaidecha W, Jannoey P and
Phanichphant S (2018) Adsorption
and Photocatalytic Processes of
Mesoporous SiO_2-Coated Monoclinic
$BiVO_4$. Front. Chem. 6:415.
doi: 10.3389/fchem.2018.00415

INTRODUCTION

Nowadays, the advanced oxidation process is known as an effective method for water purification and wastewater treatment. One of the most famous advanced oxidation process is heterogeneous photocatalysis; the contaminant (i.e., organic compounds) containing in the water and wastewater is finally degraded to carbon dioxide (Legrini et al., 1993; Mukherjee and Ray, 1999). This process can remove the organic contaminant perfectly and does not generate the second contaminant (i.e., sludge and other organic compounds) which are required the further treatment and disposal. According to the heterogeneous photocatalysis, the titanium dioxide (TiO_2) has been played a role as the important catalyst to promote the photocatalytic activity. Due to its wide band gap of 3.2 eV, the photocatalyst of TiO_2 is typically activated under the UV light (the wavelength <390 nm is required), which accounts for 45–50% of solar radiation (Linsebigler et al., 1995; Bahnemann et al., 2007; Devipriya et al., 2012). This theoretical fact becomes the limitation and non-cost-effectiveness of actual photocatalytic system for purifying the water at the site.

Another catalyst of monoclinic bismuth vanadate ($BiVO_4$) has been proposed to overcome the drawback of photocatalytic system using TiO_2 and together with enhance the photocatalytic activity during implementation. Since $BiVO_4$ has narrow band gaps of 2.4 to 2.8 eV (Kudo et al., 2001; Xie et al., 2006; Li et al., 2008), this photocatalyst can be activated by the visible light and consequences the effective use of solar energy. However, the low specific surface area and poor surface textural property are the significant disadvantages of using $BiVO_4$ as the catalyst. Its low surface area and adsorption capacity cause the low efficiency of photocatalytic system for organic contaminant removal and also the long treatment period required. Therefore, the increase in specific surface area of $BiVO_4$ catalyst is necessary prior to imply the photocatalytic system to the actual wastewater.

Recently, alternative composite materials have been synthesized by combining metal oxide and porous materials (i.e., alumina, silica, zeolites, carbon black, charcoal) (Belessi et al., 2007; Wang et al., 2012; Xing et al., 2016) with the aim of improving the specific surface area, pore structure, and photocatalytic activity of catalysts (Gan et al., 2003; Kimura et al., 2003). For example, the enhancement of Ag–doped TiO_2 photocatalytic activity was suggested by adding the mesoporous SiO_2; the excellent efficiency of methyl orange (MO) removal was achieved by 2.5 h (Roldan et al., 2015). The increasing adsorption capacity of TiO_2 catalyst was observed when the catalyst was combined with SiO_2; the adsorption capacity was increased (Hu et al., 2012). The SiO_2 addition also enhance the separation rate of electron–hole pairs under UV excitation. Further, the deposition of gold nanoparticles (Au) on the porous SiO_2-WO_3 composite can enhance the methylene blue (MB) adsorption capacity; the adsorption capacity of Au–SiO_2-WO_3 was greater than SiO_2-WO_3 and WO_3 respectively (DePuccio et al., 2015). The complete MB removal was achieved by 300 min under visible light, and the fast kinetic of MB removal was found in Au–SiO_2-WO_3 catalyst, following by Au–WO_3 and WO_3 catalysts.

As all the above mentions, this study aimed to improve the surface morphology and photocatalytic activity of $BiVO_4$ catalyst by coating SiO_2. Various analytical techniques including X–ray diffraction (XRD), transmission electron microscopy (TEM), Brunauer–Emmett–Teller (BET) and UV–vis diffuse reflectance spectra (DRS) were used to clarify the better property of $BiVO_4/SiO_2$ composite rather than $BiVO_4$ and SiO_2. Further, the performance of $BiVO_4/SiO_2$ composites on wastewater treatment was preliminary studied in the batch test under visible light irradiation, and its performance was compared to the other two materials of $BiVO_4$ and SiO_2.

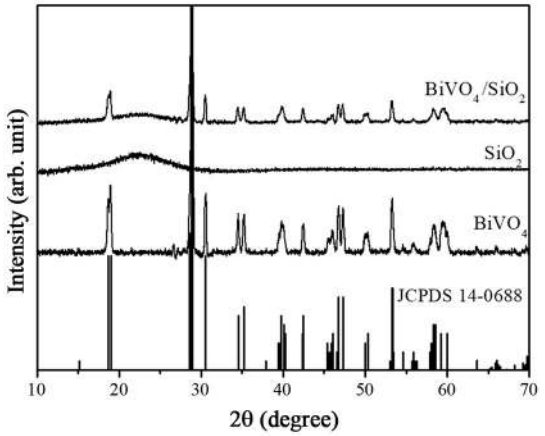

FIGURE 1 | XRD patterns of as–prepared $BiVO_4$, SiO_2, and $BiVO_4/SiO_2$.

EXPERIMENTAL PROCEDURE

All chemicals used were of analytical grade and were used as received without any further purification. The chemicals including tetraethyl orthosilicate (TEOS), bismuth (III) nitrate pentahydrate [$Bi(NO_3)_3{\cdot}5H_2O$], ammonium metavanadate (NH_4VO_3), methylene blue powder, sodium hydroxide pellet (NaOH), ammonia solution (28%) and nitric acid (37% HNO_3) were obtained from Sigma-Aldrich. All solutions were prepared with deionized water.

Preparation of SiO_2 Particles

SiO_2 particles were prepared by the sol–gel method. Ammonia solution (28%) was added in 100 mL of a mixed solution of absolute ethanol/DI water (80: 20 v/v) and stirred under ultrasonic dispersion for 60 min. Then, 20 mL of tetraethyl

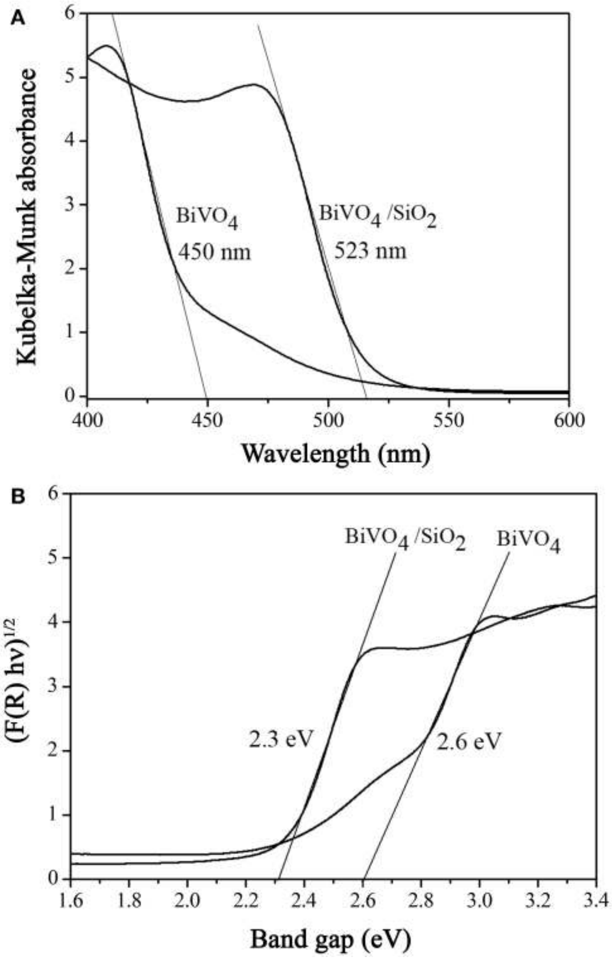

FIGURE 2 | (A) Diffuse reflectance UV–visible spectra and **(B)** the plot of adsorption function vs. photon energy for determination of band gap (E_g).

orthosilicate (TEOS) was added drop by drop to the mixed solution and stirred for 120 min at room temperature. After the reaction was homogenized, the fine particles were separated by centrifugation with typical rotating speed of 6,000 rpm for 15 min, washed by DI water and dried at 80°C for 24 h in a hot air oven. Fine particles of SiO_2 were obtained as a white powder following heat treatment at 500°C for 1 h in ambient.

Preparation of Monoclinic $BiVO_4$ and SiO_2-Coated $BiVO_4$ Composites

Monoclinic $BiVO_4$ were obtained by the co–precipitation method. Firstly, 12 mmol of bismuth (III) nitrate pentahydrate [$Bi(NO_3)_3 \cdot 5H_2O$] and the same volume of ammonium metavanadate (NH_4VO_3) were dissolved in 100 mL of 2 M nitric acid (HNO_3) under vigorous stirring. The pH of the mixed solution was adjusted to 9 by adding 3 M sodium hydroxide (NaOH). The yellow precipitate was then separated by centrifugation at 6,000 rpm for 15 min, washed thoroughly with distilled water and ethanol and finally dried in a hot air oven at 80°C for 24 h. Crystalline monoclinic $BiVO_4$ was formed after calcination at 550°C for 4 h.

$BiVO_4$-coated SiO_2 composites were also prepared by the same method for comparison with an additional step of adding SiO_2 powder to 100 mL of 2 M HNO_3.

Photocatalytic Reaction

Photocatalytic activities of the $BiVO_4$, SiO_2 and $BiVO_4/SiO_2$ composites were evaluated through degradation of methylene blue (MB) dye as a model organic pollutant under visible light. A total of 0.20 g of photocatalyst was added to 100 mL MB aqueous solution (initial concentration $C_0 = 20$ ppm) under magnetic stirring in darkness for 60 min to achieve adsorption–desorption equilibrium. The system was irradiated by three 18 W halogen lamps (Essential MR, Philips, Thailand) to investigate photocatalytic degradation. Reduction of MB concentration over time (C_t) was recorded every 15 min by measuring the intensity change of the characteristic absorption peak at 664 nm using UV–vis double beam spectroscopy (UV−6100, Mapada).

Characterisation

Crystal phase and structure of the prepared samples were characterized by powder X–ray diffraction (XRD, Philips X'Pert MPD) using Cu K_α ($\lambda = 1.54056$ Å) radiation. Morphological changes in the composite materials were monitored by transmission electron microscopy (TEM, JSM−2010, JEOL). Brunauer–Emmett–Teller (BET) measurements (Adtosorb 1 MP, Quantachrome) were performed to compare the specific surface area of the $BiVO_4$ and $BiVO_4/SiO_2$ composites. Measurement of UV–vis diffuse reflectance spectroscopy (DRS UV–vis, Shimadzu UV−3101PC) was carried out at room temperature to detect reflectance and absorbance spectra.

RESULTS AND DISCUSSION

In **Figure 1**, the broad XRD peak at $2\theta = 22$–$23°$ corresponded to the amorphous SiO_2. The XRD pattern of $BiVO_4$ without SiO_2 was assigned to the standard monoclinic $BiVO_4$ (JCPDS no. 14–0688) (Gotić et al., 2005). After coating $BiVO_4$ with

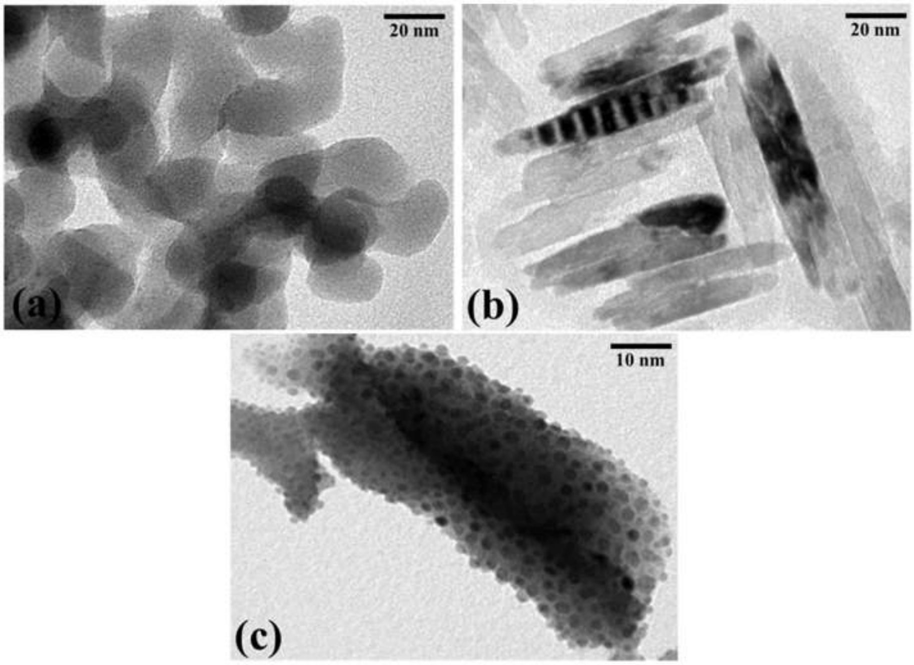

FIGURE 3 | TEM images of **(a)** SiO_2, **(b)** $BiVO_4$, and **(c)** SiO_2-coated $BiVO_4$.

SiO_2, the diffraction peaks matched well with the pure phase monoclinic $BiVO_4$ and no peaks of any other phases or impurities were recorded. However, the diffraction intensity of $BiVO_4$ decreased after coating SiO_2, because the amorphous substance had the negative effect on crystallinity. Alternatively, self–doped Si^{4+} ions in the $BiVO_4$ crystal structure might cause the decreasing crystallinity of $BiVO_4/SiO_2$ composites, and resulted in the broader peaks of the composite samples, which are similar to those reported by Phanichphant et al. (2016) for the binary composite CeO_2/SiO_2 photocatalyts and Kumar et al. for TiO_2/SiO_2 nanocomposites in solar cell applications (Arun Kumar et al., 2012).

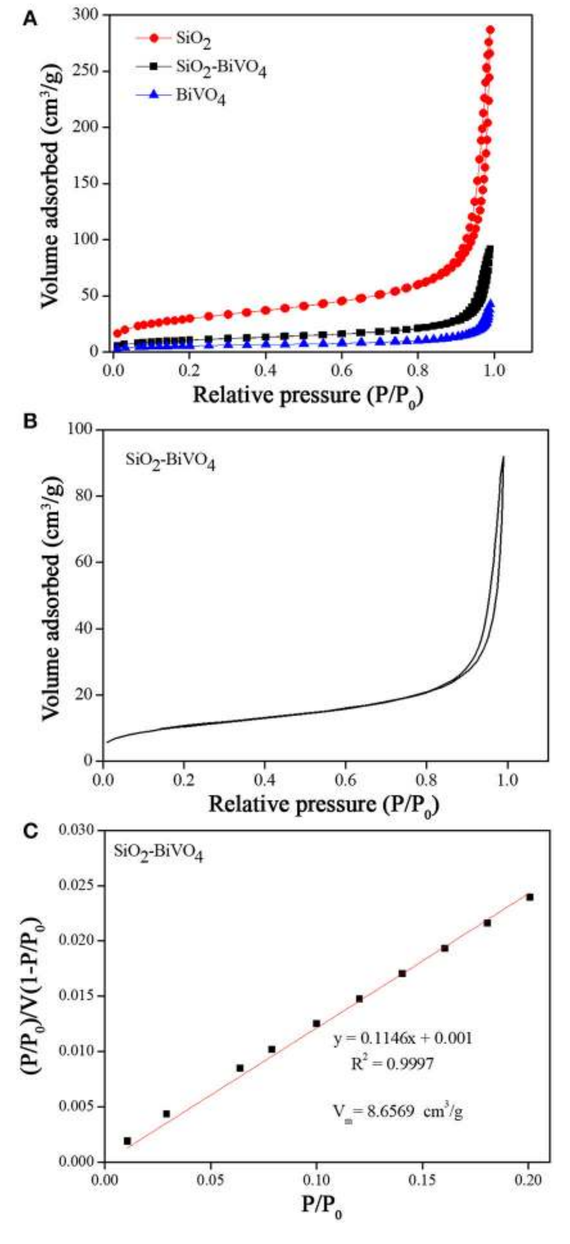

FIGURE 4 | (A), **(B)** N_2 adsorption-desorption isotherms, and **(C)** BET linear plot of relative pressure.

As shown in **Figure 2a**, the $BiVO_4$ demonstrated the absorption edge of the visible region at 450 nm, corresponding to the optical band gap (E_g) of 2.60 eV which was calculated by the Kubelka–Munk function (see **Figure 2b**) (Sirita et al., 2007). Compared to $BiVO_4/SiO_2$ composites, the value of the graph intercept was estimated at 2.30 eV, corresponding to the strong absorption edge in the visible region at 523 nm. The band gap energy of $BiVO_4$ decreased from 2.60 to 2.30 eV in the composite materials, due to the influence of Si^{4+} ions doping into the lattice of $BiVO_4$ which created the abundant doping energy levels. The estimated band gap values in this study was similar to those of $BiVO_4$ reported by Jiang et al. (2012), who prepared the $BiVO_4$ photocatalysts with different morphologies using the hydrothermal method. Liu et al. (2015) observed that the band gap energy of $BiVO_4/SiO_2$ catalyst estimated to be 2.32 eV, which was almost the same as that of calculate by this study.

The TEM images of SiO_2, $BiVO_4$ and $BiVO_4/SiO_2$ composites are presented in **Figure 3**. The SiO_2 image shows the aggregation of spherical–shaped particles with diameters ranging of 20–30 nm (**Figure 3a**), while **Figure 3b** shows the rod–like nanostructures of monoclinic $BiVO_4$ with the diameter of 10 nm and the length of 60 nm. Typical TEM images are used for characterizing the composite materials and proving the heterojunction formation between $BiVO_4$ and SiO_2, which demonstrated that the rod–like $BiVO_4$ core was covered by the SiO_2 particles growing on the surface (**Figure 3c**).

The N_2 adsorption-desorption isotherms (**Figure 4a**) show that the N_2 adsorption of $BiVO_4/SiO_2$ composites were relatively higher than that of the pure $BiVO_4$, however the value was much lower than that of the SiO_2. The specific surface areas of SiO_2, $BiVO_4/SiO_2$ composites, and $BiVO_4$ were found to be 106.9959, 37.6851, and 19.4964 m^2/g, respectively. In the meanwhile, the pore size was calculated by using the BJH method, and the results were 9.0316, 11.0776, and 11.8111 nm for SiO_2, $BiVO_4/SiO_2$, and $BiVO_4$ respectively (as summarized in **Table 1**). The surface area and pore size are positively related to the photocatalytic activity, therefore the photocatalytic activity of $BiVO_4/SiO_2$ composites were higher than that of pure $BiVO_4$. Even though the surface area of SiO_2 was higher than the $BiVO_4/SiO_2$ composite, the adsorption of pollutant by SiO_2 with high specific surface area have only the ability to transfer pollutants to alternative phases, but not completely get rid of them. Therefore, the photocatalytic process based on using the hydroxyl radicals is required in this study.

TABLE 1 | Surface properties of the prepared samples.

Sample	Specific surface area (m^2/g)	Average pore size diameter (nm)
SiO_2	106.9959	9.0316
$BiVO_4/SiO_2$	37.6851	11.0776
$BiVO_4$	19.4964	11.8111

Figure 4b shows the N_2 adsorption-desorption isotherms of $BiVO_4/SiO_2$ composites in the relative pressure (P/P_0) range 0.00–1.00. The curve exhibited Type IV isotherm characteristic with a small hysteresis loop at the relative pressure of 0.80–1.00. This indicated the existence of mesopores in the sample with the pore diameter ranging of 2–50 nm (Brunauer et al., 1940; Bae et al., 2010).

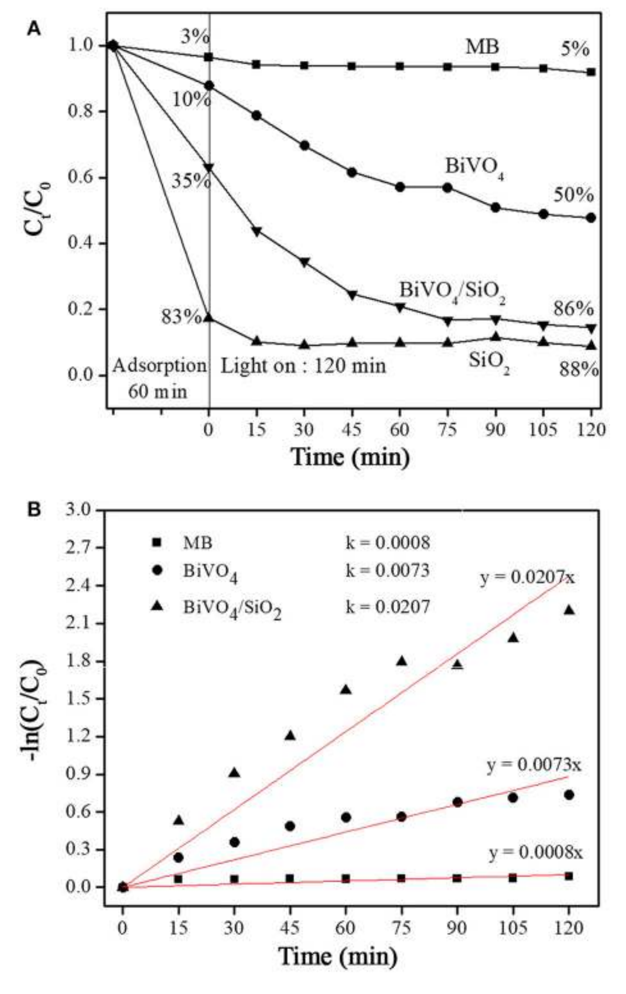

FIGURE 5 | MB concentration changes with irradiation time **(A)** C_t/C_0 and **(B)** $-\ln C_t/C_0$.

The information from the isotherm can be used to determine the specific surface area from the mathematical relations in Equation (1) and Equation (2) below (Itodo et al., 2010; Thommes et al., 2015)

$$\frac{P/P_0}{V(1-P/P_0)} = \frac{1}{V_m C} + \frac{(C-1)}{V_m C}\frac{P}{P_0} \tag{1}$$

where,

P_0, Initial pressure of N_2; P, Equilibrium pressure of N_2 adsorption; V_m, Monolayer capacity; V, Amount of N_2 adsorbed at standard temperature and pressure (STP).

$$\text{Specific Surface area} = \frac{V_m N_a \times A}{m \times 22400} \tag{2}$$

where,

A, Cross-sectional area of the adsorbed N_2; m, Adsorbate molecular weight; N_a, Avogadro's number.

The intercept and slope of the plot in **Figure 4c** were used to calculate the maximum volume of gas adsorbed at the monolayer (V_m), it was 8.6569 cm^3/g. The specific surface area was also calculated via the V_m value (see Equation 2). The result showed that the surface area of $BiVO_4/SiO_2$ composites was 37.6851 m^2/g.

Figure 5a presents the degradation efficiency of MB as a function of C_t/C_0 and visible irradiation time. The C_0 was the initial concentration of MB before irradiation and C_t was the MB concentration at the interval irradiation time (t, min). For using the SiO_2 as catalyst, the MB was removed of 83% under the dark adsorption, and only 5% of MB was further degraded under the visible light. For using the single phase monoclinic $BiVO_4$, the MB was removed around 10% under the dark adsorption, and 40% of MB was further degreased under the visible light irradiation. When the $BiVO_4/SiO_2$ composites was used, the MB removal efficiency reached 35 and 86% under

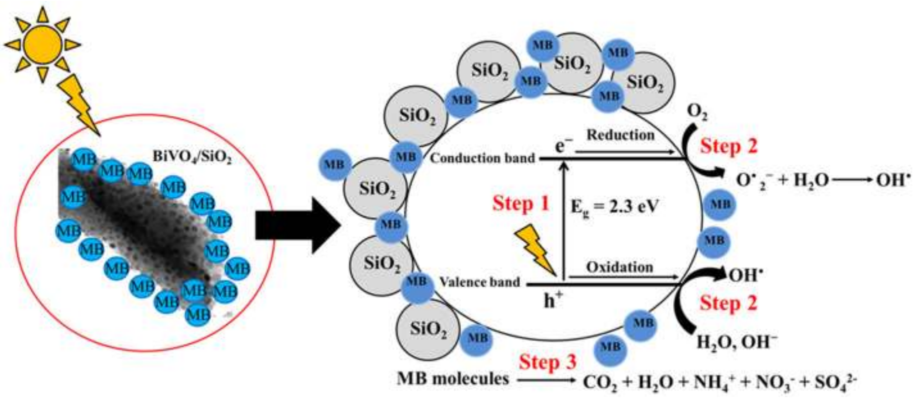

FIGURE 6 | The proposed mechanism of photogenerated charge carriers of $BiVO_4$ in $BiVO_4/SiO_2$ heterojunction.

the dark adsorption and visible light irradiation. As above explanation, the specific surface area of $BiVO_4/SiO_2$ composites were increased from $BiVO_4$, due to the SiO_2 coating. The increasing specific surface area resulted in the high adsorption of MB molecules during 60 min of the darkness, and then the adsorbed MB was continuously degraded by photocatalytic activity during visible light. These results illustrated that the photocatalytic activity of $BiVO_4$ was enhanced by coating the SiO_2 particles.

The kinetics of MB degradation was analyzed using the pseudo–first order model, which was given in Equation (3) (Yetim and Tekin, 2017). In **Figure 5b**, the correlation of–ln C_t/C_0 and t were positive with linear equation; the kinetic constant (k) were 0.0073 $\min^{-1}$ for $BiVO_4$ and 0.0207 $\min^{-1}$ for $BiVO_4/SiO_2$ composites. The kinetic constant of MB degradation using $BiVO_4/SiO_2$ composites was approximately threefold higher than that using the single phase $BiVO_4$.

$$-\ln(C_t/C_0) = kt \tag{3}$$

where k is the apparent rate constant of the pseudo–first order reaction ($\min^{-1}$).

Since the photocatalytic degradation of dyes is associated with dye adsorption onto the surface of $BiVO_4/SiO_2$. Furthermore, photocatalytic degradation occurs at or near the surface of the catalyst rather than in the bulk solution. Thus the higher photocatalytic activity of $BiVO_4/SiO_2$ is consistent with the higher adsorption of MB on the surface of $BiVO_4/SiO_2$ photocatalyst. Mesoporous SiO_2 adsorbent enriches the MB molecules around the $BiVO_4$ surface as shown in **Figure 6** and the visible–light photocatalytic activity of the $BiVO_4$ interface in the composite materials is then excited to generate electrons (e–) and holes (h^+). Subsequently, photoexcited electrons in the valance band and hole in the conduction band of $BiVO_4$ react with oxygen, water and hydroxide ions to produce free superoxide radicals ($O_2^{-\bullet}$) and hydroxyl radicals ($OH^\bullet$) as the main active oxidizing species, which then react with MB molecules during the photocatalytic process (Lin et al., 2014; Zhou et al., 2014). The final products of MB aqueous solution photocatalytic degradation are oxidized to CO_2, H_2O, CO_2, NH_4^+, NO_3^-, and SO_4^{2-} (Houas et al., 2001; Luan and Hu, 2012).

CONCLUSIONS

$BiVO_4/SiO_2$ composites consisting of spherical SiO_2 particles coated on $BiVO_4$ nanorods were successfully prepared by co–precipitation. The composites exhibited higher photocatalytic activity compared to single monoclinic $BiVO_4$ by degrading MB under visible–light irradiation due to the greater surface area of mesoporous SiO_2. Fabrication of heterogeneous semiconductors using mesoporous materials can produce promising alternative photocatalysts for wastewater treatment under light irradiation by combining adsorption and photocatalytic processes.

AUTHOR CONTRIBUTIONS

DC designed and performed the experiments and wrote the manuscript. SP, AN advised the data analysis and edited manuscript. PJ and WK advised the data analysis. All authors reviewed the approved the manuscript.

ACKNOWLEDGMENTS

This work has been supported by grant from the National Research Council of Thailand (NRCT) under Grant No. R2561B075. The Office of the Higher Education Commission and the Thailand Research Fund (TRF) under Grant No. MRG6080097 is also acknowledged for financial support.

REFERENCES

Arun Kumar, D., Merline Shyla, J., and Xavier, F. P. (2012). Synthesis and characterization of TiO_2/SiO_2 nano composites for solar cell applications. *Appl. Nanosci*. 2, 429–436. doi: 10.1007/s13204-012-0060-5

Bae, Y. S., Snurr, R. Q., and Yazaydin, O. (2010). Evaluation of the BET method for determining surface areas of MOFs and zeolites that contain ultra-micropores. *Langmuir* 26, 5479–5483. doi: 10.1021/la100449z

Bahnemann, W., Muneer, M., and Haque, M. M. (2007). Titanium dioxide-mediated photocatalysed degradation of few selected organic pollutants in aqueous suspensions. *Catal. Today* 124, 133–148. doi: 10.1016/j.cattod.2007.03.031

Belessi, V., Lambropoulou, D., and Konstantinou, I. (2007). Structure and photocatalytic performance of TiO_2/clay nanocomposites for the degradation of dimethachlor. *Appl. Catal. B*. 73, 292–299. doi: 10.1016/j.apcatb.2006.12.011

Brunauer, S., Deming, L. S., Deming, W. E., Teller, E. (1940). On a theory of the van der waals adsorption of gases. *J. Am. Chem. Soc.* 62, 1723–1732. doi: 10.1021/ja01864a025

DePuccio, D. P., Botella, P., O'Rourke, B., and Landry, C. C. (2015). Degradation of methylene blue using porous WO_3, SiO_2–WO_3, and their Au-loaded analogs: adsorption and photocatalytic studies. *ACS Appl. Mater. Interfaces* 7, 1987–1996. doi: 10.1021/am507806a

Devipriya, S. P., Yesodharan, S., and Yesodharan, E. P. (2012). Solar photocatalytic removal of chemical and bacterial pollutants from water using Pt/TiO_2-coated ceramic tiles. *Int. J. Photoenergy* 1–8. doi: 10.1155/2012/970474

Gan, L., Chen, L., and Zhang, X. (2003). Preparation of silica aerogels by non-supercritical drying. *Acta Phys. Chim. Sin.* 19, 504–508. doi: 10.3866/PKU.WHXB20030605

Gotić, M., Musić, S., Ivand, M., Šoufek, M., and Popovi, S. (2005). Synthesis and characterisation of bismuth (III) vanadate. *J. Mol. Struct*. 744, 535–540. doi: 10.1016/j.molstruc.2004.10.075

Houas, A., Lachheb, H., Ksibi, M., Elaloui, E., Guillard, C., and Herrmann, J. (2001). Photocatalytic degradation pathway of methylene blue in water. *Appl. Catal. B* 31, 145–157. doi: 10.1016/S0926-3373(00)00276-9

Hu, S., Li, F., and Fan, Z. (2012). Preparation of SiO_2-coated TiO_2 composite materials with enhanced photocatalytic activity under UV Light. *Bull. Korean Chem. Soc.* 33, 1895–1899. doi: 10.5012/bkcs.2012.33.6.1895

Itodo, A. U., Itodo, H. U., Gafar, M. K. (2010). Estimation of specific surface area using langmuir isotherm method. *J. Appl. Sci. Environ. Manage.* 14, 141–145.

Jiang, H., Meng, X., Dai, H., Deng, J., Liu, Y., Zhang, L., et al. (2012). High performance porous spherical or octapod-like single-crystalline $BiVO_4$ photocatalysts for the removal of phenol and methylene blue under visible-light illumination. *J. Hazard. Mater.* 217–218, 92–99. doi: 10.1016/j.jhazmat.2012.02.073

Kimura, I., Kase, T., Taguchi, Y., and Tanaka, M. (2003). Preparation of titania/silica composite microspheres by sol–gel process in reverse suspension. *Mater. Res. Bull*. 38, 585–597. doi: 10.1016/S0025-5408(03)00027-8

Kudo, A., Tokunaga, S., Kato, H. (2001). Selective preparation of monoclinic and tetragonal BiVO4 with scheelite structure, and their photocatalytic properties. *Chem. Mater*. 13, 4624–4628. doi: 10.1021/cm0103390

Legrini, O., Oliveros, E., and Braun, A. M. (1993). Photochemical processes for water treatment. *Chem. Rev*. 93, 671–698. doi: 10.1021/cr00018a003

Li, G., Zhang, D., and Yu, J. C. (2008). Ordered Mesoporous BiVO4 through nanocasting: a superior visible light-driven photocatalyst. *Chem. Mater*. 20, 3983–3992. doi: 10.1021/cm800236z

Lin, H., Ye, H., Chen, S., and Chen, Y. (2014). One-pot hydrothermal synthesis of BiPO4/BiVO4 with enhanced visible-light photocatalytic activities for methylene blue degradation. *RSC Adv*. 4, 10968–10974. doi: 10.1039/c3ra45288c

Linsebigler, A. L., Lu, G., and Yates, J. T. (1995). Photocatalysis on TiO2 surfaces: principles, mechanisms, and selected results. *Chem. Rev*. 95, 735–758. doi: 10.1021/cr00035a013

Liu, B., Wang, Z., Zhou, S., and He, J. (2015). Synthesis and characterization of a novel $BiVO_4/SiO_2$ nanocomposites. *Mater. Lett*. 160, 218–221. doi: 10.1016/j.matlet.2015.07.104

Luan, J., and Hu, Z. (2012). Synthesis, property characterization, and photocatalytic activity of novel visible light-responsive photocatalyst Fe2BiSbO7. *Int. J. Photoenergy* 2012, 1–11.

Mukherjee, P. S., and Ray, A. K. (1999). Application photocatalysis for treatment of industrial waste water-A short review. *Chem. Eng. Technol*. 22, 253–260. doi: 10.1002/(SICI)1521-4125(199903)22:3<253::AID-CEAT253>3.0.CO;2-X

Phanichphant, S., Nakaruk, A., and Channei, D. (2016). Photocatalytic activity of the binary composite CeO_2/SiO_2 for degradation of dye. *Appl. Surf. Sci*. 387, 214–220. doi: 10.1016/j.apsusc.2016.06.072

Roldan, M. V., Castro, Y., Pellegri, N., and Duran, A. (2015). Enhanced photocatalytic activity of mesoporous SiO_2/TiO_2 sol–gel coatings doped with Ag nanoparticles. *J. Sol–Gel Sci. Technol*. 76, 180–194. doi: 10.1007/s10971-015-3765-6

Sirita, J., Phanichphant, S., and Meunier, F. C. (2007). Quantitative analysis of adsorbate concentrations by diffuse reflectance FT-IR. *Anal. Chem*. 79, 3912–3918. doi: 10.1021/ac0702802

Thommes, M., Kaneko, K., Neimark, A. V., Olivier, J. P., Reinoso, F. R., Rouquerol, J., et al. (2015). Performance of an activated carbon-ammonia adsorption refrigeration system. *Pure Appl. Chem*. 87, 1051–1069.

Wang, X. D., Shi, F., Huang, W., and Fan, C. M. (2012). Synthesis of high quality TiO2 membranes on alumina supports and their photocatalytic activity. *Thin Solid Films* 520, 2488–2492. doi: 10.1016/j.tsf.2011.10.023

Xie, B., Zhang, H., Cai, P., Qiu, R., and Xiong, Y. (2006). Simultaneous photocatalytic reduction of Cr(VI) and oxidation of phenol over monoclinic $BiVO_4$ under visible light irradiation. *Chemosphere* 63, 956–963. doi: 10.1016/j.chemosphere.2005.08.064

Xing, B., Shi, C., Zhang, C., Yi, G., Chen, L., Guo, H., et al. (2016). Preparation of TiO2/activated carbon composites for photocatalytic degradation of RhB under UV light irradiation. *J. Nanomater*. 2016, 1–10. doi: 10.1155/2016/8393648

Yetim, T., and Tekin, T. (2017). A kinetic study on photocatalytic and sonophotocatalytic degradation of textile dyes, Period. *Polytech. Chem. Eng*. 61, 102–108.

Zhou, P., Yu, J. G., and Jaroniec, M. (2014). All-solid-state Z-scheme photocatalytic systems. *Adv. Mater*. 26, 4920–4935. doi: 10.1002/adma.201400288

Conflict of Interest Statement: The authors declare that the research was conducted in the absence of any commercial or financial relationships that could be construed as a potential conflict of interest.